

Scaling behavior of the overlap quark propagator in Landau gauge

J. B. Zhang, Patrick O. Bowman, Derek B. Leinweber and Anthony G. Williams
 CSSM Lattice Collaboration,
 Special Research Center for the Subatomic Structure of Matter
 (CSSM) and Department of Physics and Mathematical Physics,
 University of Adelaide 5005, Australia

Frederic D. R. Bonnet
 Department of Physics, University of Regina, Regina, SK, S4S 0A2, Canada
 (Dated: February 7, 2019)

The properties of the momentum space quark propagator in Landau gauge are examined for the overlap quark action in quenched lattice QCD. Numerical calculations are done on two lattices with different lattice spacings and similar physical volumes to explore the approach of the quark propagator towards the continuum limit. We have calculated the nonperturbative momentum-dependent wavefunction renormalization function $Z(p)$ and the nonperturbative mass function $M(p)$ for a variety of bare quark masses and perform a simple linear extrapolation to the chiral limit. We find the behavior of $Z(p)$ and $M(p)$ are in good agreement between the two lattices in the chiral limit.

PACS numbers: 12.38.Gc, 11.15.Ha, 12.38.Aw, 14.65.-q

I. INTRODUCTION

The quark propagator is one of the fundamental quantities in QCD. By studying the momentum-dependent quark mass function in the infrared region we can gain valuable insight into the mechanism of dynamical chiral symmetry breaking and the associated dynamical generation of mass. The ultraviolet behaviour of the propagator at large momentum can be used to extract the running quark mass [1, 2]. Furthermore, some hadron model calculations based on the Schwinger-Dyson equation formalism [3, 4] rely on models of the quark propagator. Here we have the opportunity to study it in a direct, nonperturbative fashion.

There have been several studies of the momentum space quark propagator [5, 6, 7, 8, 9] using different gauge fixing and fermion actions. Here we focus on Landau gauge fixing and the overlap fermion action and extend the previous work [9] to two lattices with different lattice spacing and very similar physical volumes. This allows us to probe the approach of the Landau gauge quark propagator to the continuum limit. The study of the overlap quark propagator in the Gribov-copy free Laplacian gauge is underway and will be reported elsewhere.

II. QUARK PROPAGATOR ON THE LATTICE

In a covariant gauge in the continuum, the renormalized Euclidean space quark propagator must have the form

$$S(\not{p}) = \frac{1}{i\not{p}A(\not{p}^2) + B(\not{p}^2)} = \frac{Z(\not{p}^2)}{i\not{p} + M(\not{p}^2)}; \quad (1)$$

where \not{p} is the renormalization point. The renormalization point boundary conditions are chosen to be

$$Z(\not{p}^2) \rightarrow 1 \quad M(\not{p}^2) \rightarrow m(\not{p}^2); \quad (2)$$

where $m(\not{p}^2)$ is the renormalized quark mass at the renormalization point. The functions $A(\not{p}^2)$ and $B(\not{p}^2)$, or alternatively $Z(\not{p}^2)$ and $M(\not{p}^2)$, contain all of the nonperturbative information of the quark propagator. Note that $M(\not{p}^2)$ is renormalization point independent, i.e., since $S(\not{p})$ is multiplicatively renormalizable all of the renormalization-point dependence is carried by $Z(\not{p}^2)$. For sufficiently large momenta the effects of dynamical chiral symmetry breaking become negligible for nonzero current quark masses, i.e., for large \not{p} and $m \neq 0$ we have $m(\not{p}^2) \rightarrow m$ where m is the usual current quark mass of perturbative QCD at the renormalization point.

When all interactions for the quarks are turned off, i.e., when the gluon field vanishes, the quark propagator has its tree-level form

$$S^{(0)}(\not{p}) = \frac{1}{i\not{p} + m^0}; \quad (3)$$

where m^0 is the bare quark mass. When the interactions with the gluon field are turned on we have

$$S^{(0)}(p) \neq S^{\text{bare}}(a;p) = Z_2(\mu;a)S(\mu;p); \quad (4)$$

where a is the regularization parameter (i.e., the lattice spacing here) and $Z_2(\mu;a)$ is the quark wave-function renormalization constant chosen so as to ensure $Z_2(\mu;a^2) = 1$. For simplicity of notation we suppress the a -dependence of the bare quantities.

On the lattice we expect the bare quark propagators, in momentum space, to have a similar form as in the continuum, except that the $O(4)$ invariance is replaced by a 4-dimensional hypercubic symmetry on an isotropic lattice. Hence, the inverse lattice bare quark propagator takes the general form

$$(S^{\text{bare}})^{-1}(p) = i \sum_{\mu=1}^4 C_{\mu}(p) \gamma_{\mu} + B(p); \quad (5)$$

We use periodic boundary conditions in the spatial directions and anti-periodic in the time direction. The discrete momentum values for a lattice of size $N_i^3 \times N_t$, with $n_i = 1; \dots; N_i$ and $n_t = 1; \dots; N_t$, are

$$p_i = \frac{2}{N_{ia}} n_i \frac{N_i}{2}; \quad \text{and} \quad p_t = \frac{2}{N_{ta}} n_t \frac{1}{2} - \frac{N_t}{2}; \quad (6)$$

Defining the bare lattice quark propagator as

$$S^{\text{bare}}(p) = i \sum_{\mu=1}^4 C_{\mu}(p) \gamma_{\mu} + B(p); \quad (7)$$

we perform a spinor and color trace to identify

$$C_{\mu}(p) = \frac{i}{4N_c} \text{tr}[\gamma_{\mu} S^{\text{bare}}(p)] \quad \text{and} \quad B(p) = \frac{1}{4N_c} \text{tr}[S^{\text{bare}}(p)]; \quad (8)$$

The inverse propagator is

$$\begin{aligned} (S^{\text{bare}})^{-1}(p) &= \frac{1}{i \sum_{\mu=1}^4 C_{\mu}(p) \gamma_{\mu} + B(p)} \\ &= \frac{i \sum_{\mu=1}^4 C_{\mu}(p) \gamma_{\mu} + B(p)}{C^2(p) + B^2(p)}; \end{aligned} \quad (9)$$

where $C^2(p) = \sum_{\mu=1}^4 (C_{\mu}(p))^2$. From Eq. (5) we identify

$$C_{\mu}(p) = \frac{C(p)}{C^2(p) + B^2(p)} \quad \text{and} \quad B(p) = \frac{B(p)}{C^2(p) + B^2(p)}; \quad (10)$$

At tree-level, i.e., when all the gauge links are set to the identity, the inverse bare lattice quark propagator becomes the tree-level version of Eq. (5)

$$(S^{(0)})^{-1}(p) = i \sum_{\mu=1}^4 C^{(0)}_{\mu}(p) \gamma_{\mu} + B^{(0)}(p); \quad (11)$$

We calculate $S^{(0)}(p)$ directly by setting the links to unity in the coordinate space quark propagator and taking its Fourier transform. It is then possible to identify the appropriate kinematic lattice momentum directly from the definition

$$q_{\mu} = C^{(0)}_{\mu}(p) = \frac{C^{(0)}(p)}{(C^{(0)}(p))^2 + (B^{(0)}(p))^2}; \quad (12)$$

This is the starting point for the general approach to tree-level correction developed in earlier studies of the gluon propagator [10, 11] and the quark propagator [5, 6, 7]. For overlap quarks no tree-level correction is needed [9]. This feature is a major advantage of the overlap formalism.

Having identified the appropriate kinematical lattice momentum q , we can now define the bare lattice propagator as

$$S^{\text{bare}}(p) = \frac{1}{i\mathbb{q}A(p) + B(p)} = \frac{Z(p)}{i\mathbb{q} + M(p)} = Z_2(\mathbb{q}; a) S(\mathbb{q}; p) \quad (13)$$

and the lattice version of the renormalized propagator in Eq. (1)

$$S(\mathbb{q}; p) = \frac{1}{i\mathbb{q}A(\mathbb{q}; p) + B(\mathbb{q}; p)} = \frac{Z(\mathbb{q}; p)}{i\mathbb{q} + M(p)} : \quad (14)$$

The overlap fermion formalism [12, 13] realizes an exact chiral symmetry on the lattice and is automatically $O(a)$ improved, since any $O(a)$ error would necessarily violate chiral symmetry [14]. The massless coordinate-space overlap-Dirac operator can be written in dimensionless lattice units as [15]

$$D(0) = \frac{1}{2} [1 + \gamma_5 H_a] ; \quad (15)$$

where H_a is an Hermitian operator that depends on the background gauge field and has eigenvalues ± 1 . Any such $D(0)$ is easily seen to satisfy the Ginsparg-Wilson relation [16]

$$f_{\gamma_5} D(0) g = 2 D(0) \gamma_5 D(0) : \quad (16)$$

It follows easily that $f_{\gamma_5} D^{-1}(0) g = 2 \gamma_5$ and by defining $\mathcal{D}^{-1}(0) = D^{-1}(0) - 1$ we see that the Ginsparg-Wilson relation can also be expressed in the form

$$f_{\gamma_5} \mathcal{D}^{-1}(0) g = 0 : \quad (17)$$

The standard choice of $H_a(x; y)$ is $H_a = (H_w) - H_w = \mathbb{H}_w \mathbb{J} = H_w = (\mathbb{H}_w^\dagger H_w)^{1/2}$, where $H_w(x; y) = \gamma_5 D_w(x; y)$ is the Hermitian Wilson-Dirac operator and where D_w is the usual Wilson-Dirac operator on the lattice. However, in the overlap formalism the Wilson mass parameter m_w is negative.

In the present work we use the mean-field improved Wilson-Dirac operator, which can be written as

$$D_w(x; y) = \frac{u_0}{2} \sum_{x, y} \sum_{\mu} \left((x) - \frac{U_\mu(x)}{u_0} \right) \gamma_\mu \delta_{y, x + \hat{\mu}} + (x + \hat{\mu}) - \frac{U_\mu^\dagger(x + \hat{\mu})}{u_0} \gamma_\mu \delta_{y, x - \hat{\mu}} : \quad (18)$$

We see that this is equivalent to the standard Wilson-Dirac operator with the identification of the mean-field improved coefficient u_0 [9]. It is $U = u_0$ that has a more convergent expansion around the identity than the links U themselves. The negative Wilson mass ($m_w a$) is then related to this improved by

$$\frac{u_0}{2(m_w a) + (1 - c)} : \quad (19)$$

The Wilson parameter is chosen to be $r = 1$ in our numerical simulations.

The massless overlap quark propagator is given by

$$S^{\text{bare}}(0) = \mathcal{D}_c^{-1}(0) = D_c^{-1}(0) = \frac{1}{2m_w} = \frac{1}{2m_w} D^{-1}(0) - 1 = \frac{1}{2m_w} \mathcal{D}^{-1}(0) : \quad (20)$$

This definition of the massless overlap quark propagator follows from the overlap formalism [17] and ensures that the massless quark propagator anticommutes with γ_5 , i.e., $f_{\gamma_5} S^{\text{bare}}(0) g = 0$ just as it does in the continuum [15]. At tree-level the momentum-space form of the massless propagator defines the kinematical lattice momentum q , i.e., we set the links to one such that we have for the momentum-space massless quark propagator

$$S^{\text{bare}}(0; p) = \mathcal{D}_c^{-1}(0; p) \neq S^{(0)}(0; p) = \frac{1}{i\mathbb{q}} ; \quad (21)$$

where p is the discrete lattice momentum defined in Eq. (6) and q is the kinematical lattice momentum defined in Eq. (12). We can obtain q numerically in this way from the tree-level massless quark propagator [9]. A derivation of the analytic form of q and of the overlap quark dispersion relation can also be found in Ref. [9].

Having identified the massless quark propagator in Eq. (20), we can construct the massive overlap quark propagator by simply adding a bare mass to its inverse, i.e.,

$$(S^{\text{bare}})^{-1}(m^0) = (S^{\text{bare}})^{-1}(0) + m^0 : \quad (22)$$

Hence, at tree-level we have for the massive, momentum-space overlap quark propagator

$$S^{\text{bare}}(m^0; p) = S^{(0)}(m^0; p) = \frac{1}{i\cancel{p} + m^0} \quad (23)$$

and the reason that the overlap quark propagator needs no tree-level correction beyond identifying q is now clear. In the case of non-zero bare quark mass, the overlap operator can be defined as [15]

$$D(\cdot) = (1 - \gamma_5)D(0) + \frac{1}{2} [1 + \gamma_5 H_a] ; \quad (24)$$

where the quark mass parameter

$$\frac{m^0}{2m_w} ; \quad (25)$$

and the overlap quark propagator is given by the equation

$$S^{\text{bare}}(m^0) = D_c^{-1}(\cdot) ; \quad (26)$$

where

$$D_c^{-1}(\cdot) = \frac{1}{2m_w} D^{-1}(\cdot) \quad \text{and} \quad D^{-1}(\cdot) = \frac{1}{1} D^{-1}(\cdot) - 1 : \quad (27)$$

We see that the massless limit, $m^0 \rightarrow 0$, implies that $\gamma_5 \rightarrow 0$ and $D(\cdot) \rightarrow D(0)$, $D_c^{-1}(\cdot) \rightarrow D_c^{-1}(0)$ and $D_c^{-1}(\cdot) \rightarrow D_c^{-1}(0)$. For non-negative bare mass m^0 we require $\gamma_5 \geq 0$. In order that the above expressions and manipulations be well-defined we must have $\gamma_5 < 1$. Hence, $0 \leq \gamma_5 < 1$ defines the allowable range of bare masses.

III. NUMERICAL RESULTS

Here we work on two lattices with different lattice spacing, a , and very similar physical volumes, created using a tadpole improved plaquette plus rectangle (Lüscher-Weisz [19]) gauge action through the pseudo-heatbath algorithm [20]. For each lattice size, we use 50 configurations. Lattice parameters are summarized in Table I. The lattice spacing is determined from the static quark potential with a string tension $\sigma = 440 \text{ MeV}$ [18].

TABLE I: Lattice parameters.

Action	Volume	N_{Therm}	N_{Sample}	a (fm)	u_0	Physical Volume (fm ⁴)
Improved	12 ³ × 24	5000	500	4.60	0.125	1.5 ³ × 3.00
Improved	8 ³ × 16	5000	500	4.286	0.194	1.552 ³ × 3.104

The gauge field configurations are gauge fixed to the Landau gauge using a Conjugate Gradient Fourier Acceleration [21] algorithm with an accuracy of $\sum_j |A(x)|^2 < 10^{-12}$. We use an improved gauge-fixing scheme to minimize gauge-fixing discretization errors. A discussion of the functional and method for improved Landau gauge fixing can be found in Ref. [22].

Our numerical calculation begins with an evaluation of the inverse of $D(\cdot)$, where $D(\cdot)$ is defined in Eq. (24) and using $H_a = (H_w)$ for each gauge configuration in the ensemble. We then calculate Eq. (26) for each configuration and take the ensemble average to obtain $S^{\text{bare}}(x; y)$. The discrete Fourier transform of this naturally gives the momentum-space bare quark propagator, $S^{\text{bare}}(p)$, for the bare quark mass m^0 . Our calculations used $\gamma_5 = 0.19$ for lattice 1 (12³ × 24) and since at tree level $\gamma_5 = 1/8$, we then have $m_w a = 1.661$. For lattice 2 (8³ × 16), we choose $\gamma_5 = 0.1864$ to give $m_w a = 1.661$. We calculate at ten quark masses specified by $\gamma_5 = 0.024, 0.028, 0.032, 0.040, 0.048, 0.060, 0.080, 0.100, 0.120$, and 0.140 for lattice 1. This corresponds to bare masses in physical units of $m^0 = 2 m_w = 126$,

147, 168, 210, 252, 315, 420, 524, 629, and 734 MeV respectively. For lattice 2, we choose 10 mass parameters μ_i so as to make $m_i^0 = 2 \mu_{i,w}$ the same as on lattice 1.

The results of lattice 1 are presented in detail in Ref. [9]. It is satisfying that the results of lattice 2 are similar to those of lattice 1. Here we are focusing on the comparison of the results on these two lattices. All data has been cylinder cut [10]. First we present the results for finite quark masses. The results for the mass function $M(p)$ for the two lattices at $m^0 = 168$ MeV are plotted in Fig. 1. The comparison of results for the other masses are very similar. We can clearly see that if the mass function $M(p)$ is plotted against the discrete lattice momentum p , the results of the two lattices are in good agreement with each other. But if the mass function $M(p)$ is plotted against kinematical lattice momentum q , the agreement of the two is less satisfactory. The results for the renormalization function $Z(p)$ of the two lattices at $m^0 = 168$ MeV is plotted in Fig. 2. The renormalization point is $\mu = 3.9$ GeV. If the renormalization function $Z(p)$ is plotted against kinematical lattice momentum q , the results on the two lattices are in reasonably good agreement. In the $Z^{(R)}(p)$ versus q plot in Fig. 2 there is a small difference remaining in the infrared which should be studied further with another lattice spacing in the future.

Thus we have resolved one of the key questions raised in the studies of Ref. [9], i.e., we see that the continuum limit appears to be approached most rapidly when $Z(p)$ and $M(p)$ are plotted against q and p respectively. Since the regularization parameter, a , is different on the two lattices, selecting the same m^0 is not exactly equivalent to selecting the same current quark mass. For our purposes, however, this mismatch will be a small effect, as evidenced by the excellent agreement in the infrared for $M(p)$. This small mismatch of bare masses can be avoided by comparing the two lattices in the chiral limit.

The chiral extrapolated data are obtained from a simple linear chiral extrapolation. The mass function $M(p)$ for the two lattices in the chiral limit is plotted in Fig. 3, as anticipated from the case of finite m^0 , when the mass function $M(p)$ is plotted against the discrete lattice momentum p the results of the two lattice are in good agreement. The results for the renormalization function $Z(p)$ of the two lattices in the chiral limit is plotted in Fig. 4. Again it seems that when the renormalization function $Z(p)$ is plotted against the kinematical lattice momentum q , the results on the two lattices are in good agreement. We attribute the relatively small discrepancies in $Z^{(R)}(p)$ versus q and $M(p)$ versus p between our two lattices to that fact that our lattice 2 has a lattice spacing of $a = 0.194$ fm, which is somewhat coarse.

In the chiral limit, in the continuum, the asymptotic quark mass function has the form

$$M(p^2)^{p^2 \rightarrow 1} = \frac{4^{-2} d_M}{3} \frac{h^{-1}}{[\ln(\mu^2 = \frac{2}{Q_{CD}})]^{d_M}} \frac{[\ln(p^2 = \frac{2}{Q_{CD}})]^{d_M - 1}}{p^2} \quad (28)$$

(see Ref. [3], Eq. (6.15)) where the anomalous dimension of the quark mass is $d_M = 12 = (33 - 2N_f)$ for N_f quark flavors ($N_f = 0$ in the present case) and we use $\frac{M_{QCD}^{OM}}{Q_{CD}} = 691$ MeV. The dependence of $M(p^2)$ on the renormalization point is cancelled by the dependence of the condensate, maintaining the renormalization point invariance of the mass function. Using momentum p , this form was fit to the data from the finer lattice, resulting in a value for the condensate

$$h^{-1} = (273 \pm 50 \text{ MeV})^3: \quad (29)$$

This is in excellent agreement with the value extracted from the Aqtad action using the same method [7]. If the momentum q is employed, which we have already seen to be less desirable, then the very different result of $h^{-1} = (468 \pm 37 \text{ MeV})^3$ is obtained, which again suggests that for the overlap quark action it is most appropriate to plot $M(p)$ versus p .

We also perform a fit to the data using the ansatz of Ref. [7],

$$M(q^2) = \frac{C^{-2(1)}}{q^2 + \frac{1}{2}}: \quad (30)$$

in the chiral limit. This form is finite at zero four-momentum and has been seen to provide a good description of the infrared behavior of the quark mass function [5, 7]. The consistency of the fit parameters, shown in Table II, shows us again the good scaling of the overlap action. These results are also consistent with those obtained from the Aqtad action [7], which is another indicator that our choice of momentum is correct for this action.

IV. SUMMARY AND OUTLOOK

In this paper we explore the nonperturbative quark propagator on Luscher-W eisz $O(a^2)$ tadpole-improved quenched lattice configurations and the overlap fermion operator with the Wilson overlap kernel. The momentum space quark

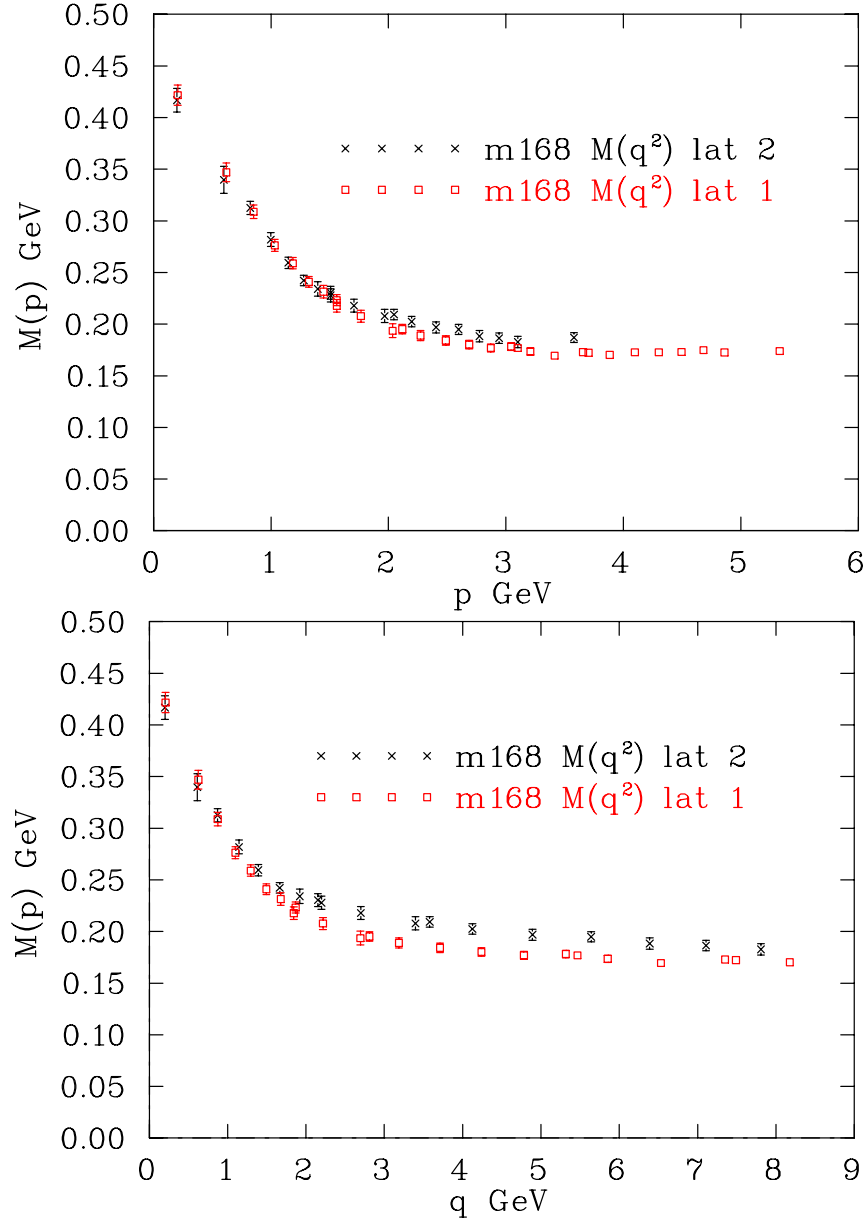


FIG. 1: The mass function $M(p)$ corresponding to a bare mass $m^0 = 168$ MeV is shown for our two lattices. A cylinder cut has been used [10]. In the upper part of the figure $M(p)$ is plotted against the discrete lattice momentum p , whereas in the lower part it is plotted against the kinematical momentum q . The results suggest that we most rapidly approach the continuum limit by plotting $M(p)$ against p .

propagator was calculated in $O(a^2)$ improved Landau gauge on two lattices with different lattice spacing a and very similar physical volumes in order to explore its approach to the continuum limit. We calculated the nonperturbative momentum-dependent wavefunction renormalization $Z(p)$ and the nonperturbative mass function $M(p)$ for a variety of bare quark masses. We also performed a simple linear extrapolation to the chiral limit. As previously anticipated [9], the continuum limit for $Z(p)$ is approached most rapidly when it is plotted against the kinematical lattice momentum q , whereas for the quark mass function, $M(p)$, plotting against the discrete lattice momentum p provides the most rapid approach to the continuum limit. The agreement between the two lattices suggests that we are close to the continuum limit, and it seems reasonable to conclude that our finer lattice results [9] are a good approximation to this limit.

Future work should test our conclusions and further explore the continuum limit with one or more additional finer lattice spacings. In addition, a variety of volumes should be studied to explore the infinite volume limit. One can also use other kernels in the overlap fermion formalism, e.g., using a fat-link irrelevant clover (FLIC) action [23] as the

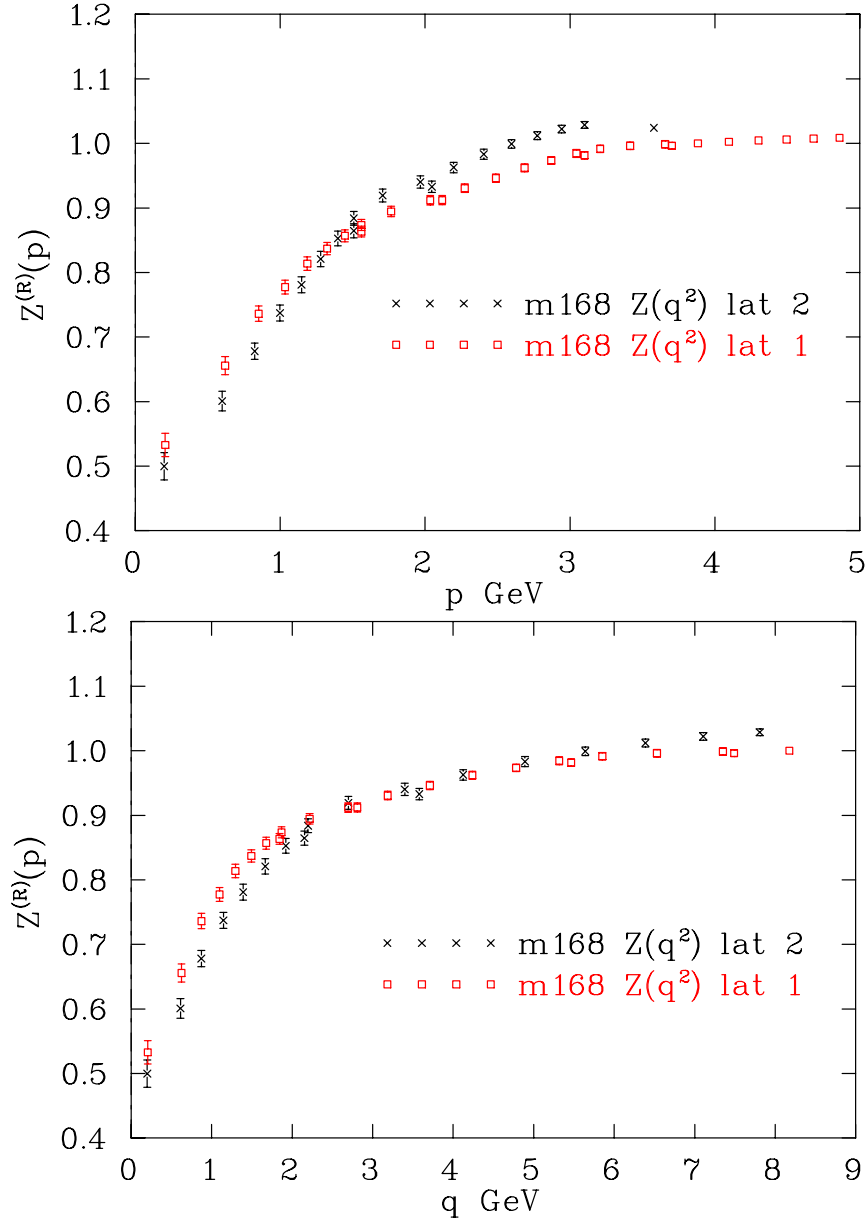


FIG. 2: The momentum-dependent wavefunction renormalization function $Z^{(R)}(p) = Z(\vec{p}; p)$ for renormalization point $\mu = 3.9$ GeV (on the p -scale) for the case of bare mass $m^0 = 168$ MeV. A cylinder cut has been used [10]. In the upper part of the figure $Z^{(R)}(p)$ is plotted against the discrete lattice momentum p whereas in the lower part it is plotted against the kinematical momentum q . The results suggest that we most rapidly approach the continuum limit by plotting $Z^{(R)}(p)$ against q .

overlap kernel [24, 25] in order to further establish the robustness of our conclusions and to provide more accurate data. These studies are currently underway and results will be reported elsewhere.

V. ACKNOWLEDGEMENT

Support for this research from the Australian Research Council is gratefully acknowledged. This work was carried out on the Orion supercomputer at University of Adelaide. We thank Paul Coddington and Francis Vaughan for

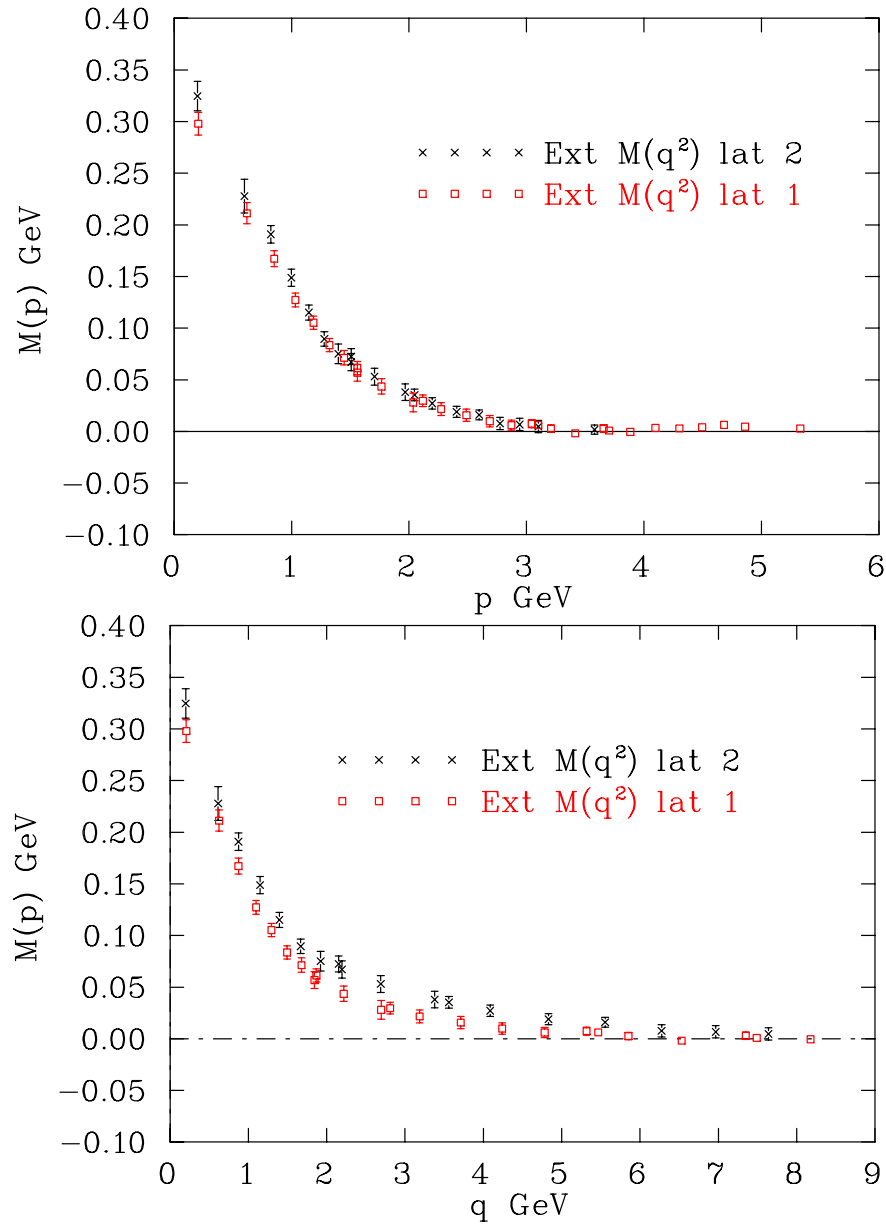


FIG. 3: The mass function $M(p)$ from a linear extrapolation to the chiral limit is shown for our two lattices. In the upper part of the figure $M(p)$ is plotted against the discrete lattice momentum p , whereas in the lower part it is plotted against the kinematical momentum q . The results again suggest that we most rapidly approach the continuum limit by plotting $M(p)$ against p .

supercomputer support.

-
- [1] S. Aoki et al, Phys. Rev. Lett. 82, 4392 (1999).
 - [2] D. Becirevic, V. Gimenez, V. Lubicz and G. Martinelli, Phys. Rev. D, 61, 114507 (2000).
 - [3] C. D. Roberts and A. G. Williams, Prog. Part. Nucl. Phys. 33, 477 (1994).
 - [4] R. Alkofer and L. von Smekal, Phys. Rept. 353, 281 (2001).
 - [5] J. I. Skullerud and A. G. Williams, Phys. Rev. D 63, 054508 (2001); Nucl. Phys. Proc. Suppl. 83, 209 (2000).
 - [6] J. Skullerud, D. B. Leinweber and A. G. Williams, Phys. Rev. D 64, 074508 (2001).
 - [7] P. O. Bowman, U. M. Heller and A. G. Williams, Nucl. Phys. B (Proc. Suppl.) 106, 820 (2002).
 - [8] T. Blum et al, Phys. Rev. D 66, 014504 (2002).

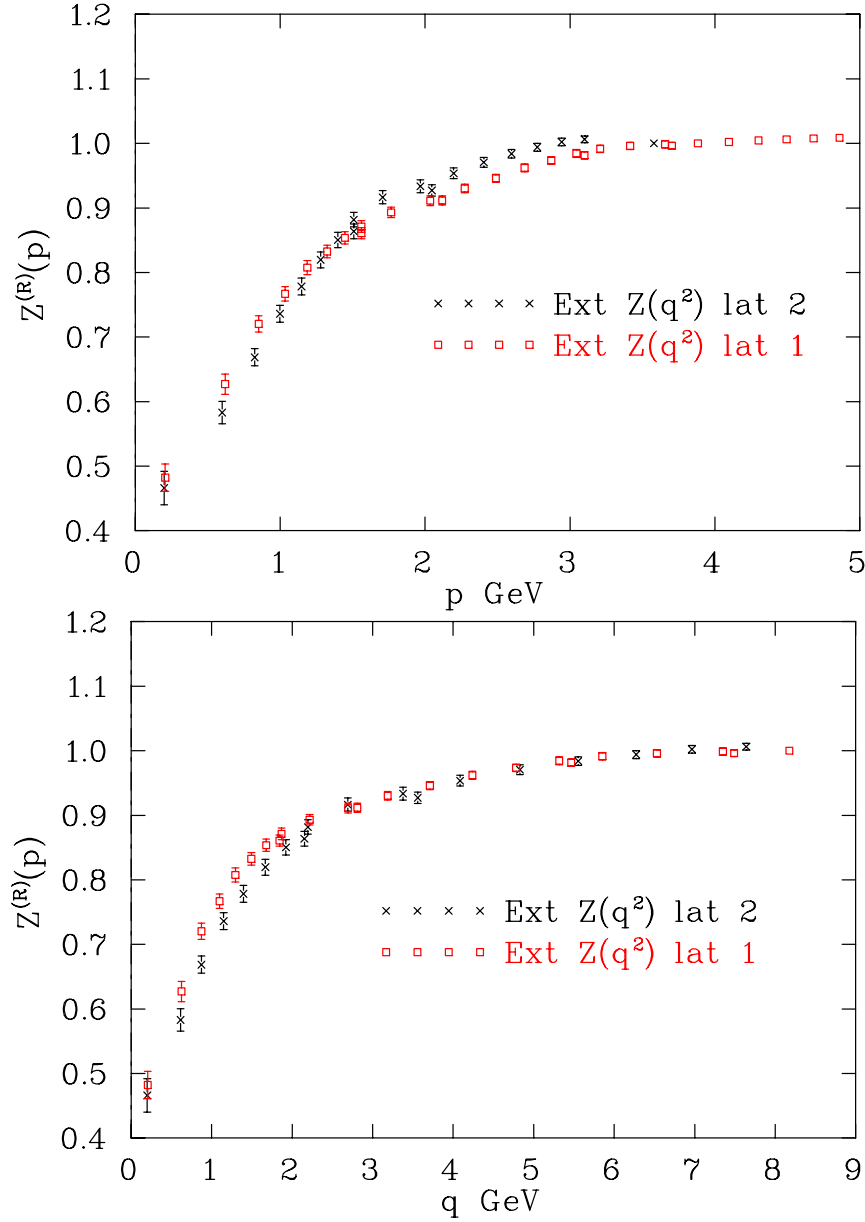


FIG. 4: The momentum-dependent wavefunction renormalization function $Z^{(R)}(p) = Z(\vec{p}; p)$ for renormalization point $\mu = 3.9$ GeV (on the p -scale) from a linear extrapolation to the chiral limit. In the upper part of the figure $Z^{(R)}(p)$ is plotted against the discrete lattice momentum p whereas in the lower part it is plotted against the kinematical momentum q . The results again suggest that we most rapidly approach the continuum limit by plotting $Z^{(R)}(p)$ against q .

- [9] F.D.R. Bonnet, P.O. Bowman, D.B. Leinweber, A.G. Williams and J.B. Zhang, Phys.Rev.D 65, 114503 (2002).
- [10] D.B. Leinweber, J.I. Skullerud, A.G. Williams and C. Parrinello, Phys.Rev.D 60, 094507 (1999); Erratum -ibid.D 61, 079901 (1999); D.B. Leinweber, J.I. Skullerud, A.G. Williams and C. Parrinello Phys.Rev.D 58, 031501 (1998).
- [11] F.D.R. Bonnet, P.O. Bowman, D.B. Leinweber, A.G. Williams and J.M. Zanotti, Phys.Rev.D 64, 034501 (2001). F.D.R. Bonnet, P.O. Bowman, D.B. Leinweber and A.G. Williams, Phys.Rev.D 62, 051501 (2000).
- [12] R. Narayanan and H. Neuberger Nucl. Phys. B 443, 305 (1995).
- [13] H. Neuberger, Phys. Lett. B 427, 353 (1998).
- [14] F. Niedermayer, Nucl. Phys. Proc. Suppl. 73, 105 (1999).
- [15] R.G. Edwards, U.M. Heller, and R. Narayanan, Phys.Rev.D 59, 094510 (1999).
- [16] P.H. Ginsparg and K.G. Wilson, Phys.Rev.D 25, 2649 (1982).
- [17] R. Narayanan and H. Neuberger, Nucl. Phys. B 443, 305 (1995).
- [18] F.D.R. Bonnet, D.B. Leinweber, A.G. Williams and J.M. Zanotti, Symmetries and improvement in the static quark potential, hep-lat/9912044.

TABLE II: Best-fit parameters for the ansatz, Eq. (30), in physical units. These two lattices are closely matched in physical volume, so the good agreement in fitting parameters further indicates that the overlap action provides excellent scaling.

	$c^{1=3}$ (MeV)	(MeV)		$M(0)$ (MeV)
4.286	654 (14)	953 (36)	1.41 (10)	308 (14)
4.60	644 (15)	964 (45)	1.53 (12)	287 (15)

[19] M. Luscher and P. Weisz, Commun. Math. Phys. 97, 59 (1985).

[20] N. Cabibbo & E. Marinari, Phys. Lett. B 119, 387 (1982).

[21] A. Cucchieri and T. Mendes, Phys. Rev. D 57, 3822 (1998).

[22] F. D. R. Bonnet, P. O. Bowman, D. B. Leinweber, A. G. Williams and D. G. Richards, Austral. J. Phys. 52, 939 (1999).

[23] J. M. Zanotti et al. [CSSM Lattice Collaboration], Phys. Rev. D 65, 074507 (2002)

[24] W. Kamleh, D. Adams, D. B. Leinweber and A. G. Williams, Nucl. Phys. Proc. Suppl. 109, 81 (2002), and Phys. Rev. D 66, 014501 (2002).

[25] W. Kamleh, D. J. Kusterer, D. B. Leinweber and A. G. Williams, hep-lat/0209156.